International Journal of Innovative
Computing, Information and Control
Volume **12**, Number **6**, December **2016**

ICIC International ©2016 ISSN 1349-4198
pp. 1791–1808

AUTOCORRELATION FUNCTION AND THE POWER SPECTRUM CALCULATION FOR PRODUCTION PROCESSES

Kenji Shirai[1] and Yoshinori Amano[2]

[1]Faculty of Information Culture
Niigata University of International and Information Studies
3-1-1, Mizukino, Nishi-ku, Niigata 950-2292, Japan
shirai@nuis.ac.jp

[2]Kyohnan Elecs Co., LTD.
8-48-2, Fukakusanishiura-cho, Fushimi-ku, Kyoto 612-0029, Japan
y_amano@kyohnan-elecs.co.jp

Received April 2016; revised August 2016

Abstract. *Our motivation is to clarify the reason why the stochastic resonance occurs in production system. The noises regard as the probability element that the worker affects the process progress, or the supply chain has an impact in the process. The stochastic resonance represents the relationship between the volatility of the working ability as the noise intensity and the throughput. This study is part of an ongoing report on stochastic resonance; it describes the auto-correlation function based on the self-similarity of the production process. When the probability intensity coefficient in the explicit solution of the autocorrelation function is small, the influence of the phase difference is small. By contrast, when the probability intensity coefficient is large, the influence is great and the form of the phase difference is temporally shifted in the right direction of the border. The stochastic resonance is observed. In addition, we have calculated the explicit equation of the power spectrum. As a result, the correlation function spectrum of the process phase difference is known to have a Lorentz-type spectrum. We are calculating the autocorrelation function of the final processes in consideration of the previous processes because the previous processes substantially affect throughput. The autocorrelation function is extremely important in evaluating the production flow process.*

Keywords: Stochastic resonance, Autocorrelation function, Transition probability density function, Power spectrum, Probability throughput

1. **Introduction.** Based on mathematical and physical understandings of production engineering, we are conducting research aiming at establishing an academic area called mathematical production engineering. As our business size is a small-to-medium-sized enterprise, human intervention constitutes a significant part of the production process, and revenue can sometimes be greatly affected by human behavior. Therefore, when considering human intervention from outside companies, a deep analysis of the production process and human collaboration is necessary to understand the potential negative effects of such intervention.

With respect to mathematical modeling of deterministic systems in our studies, a physical model of the production process was constructed using a one-dimensional diffusion equation in 2012 [1]. Especially, many concerns that occur in the supply chain are major problems facing production efficiency and business profitability.

With respect to the analysis of production processes based on physics in our studies, we have clarified that phenomena such as power-law distributions, self-similarity, phase transitions, and on-off intermittency can occur in production processes [5, 6, 7, 8, 9].

On the other hand, there is a famous theory of constraints (TOC) that describes the importance of avoiding bottlenecks in production processes [10]. We proposed that small fluctuations in an upstream subsystem appear as large fluctuations in the downstream (the so-called bullwhip effect) [13]. The bullwhip effect generates a large gap between the demand forecasts of the market and suppliers. Large fluctuations can be suppressed by the following mechanisms.

(1) Reducing the lead time, improving the throughput, and synchronizing the production process by the TOC.
(2) Sharing the demand information and performing mathematical evaluations.
(3) Analyzing the reduction and fluctuating demands of the subsystem (using nonlinear vibration theory).
(4) Basing the inventory management approach on stochastic demand.

We consider internal and external forces as two parameters in the production system. Rather than selecting the ratio between lead time and throughput that optimizes an individual's productivity, we select the parameters that achieve overall synchronization [4, 12]. In our previous study of a production system involving worker intervention, the specific abilities of workers required empirical analysis. To optimize typical modern production systems, we must recognize the importance of biological fluctuations. For example, the following aims typify technical innovation in the engineering industries:

(1) Detecting a small signal using the noise in the force;
(2) Synchronizing the circuit groups using the noise power.

With respect to stochastic resonance (SR) in our studies, we utilized in physical systems such electronic circuits, and even in biological systems such as neurotransmission; as a result, the same phenomenon has been confirmed [17, 18]. However, there have been no reports on application of SR in production processes for the improvement of throughput. Accordingly, we present the improvement of throughput in production processes using SR in the present study.

Moreover, worker productivity in a high-mix, low-volume production process is optimized for the market demand, rather than the mass production process. To demonstrate the effectiveness of the throughput when the worker productivity is analyzed in this manner, we extract the probability distribution of the productivities of workers in a real production firm. Analyzing the actual results, we ascertain the probabilities of human factors in a production process.

Fujisaka and colleagues modeled the production process as a circuit system with an annular structure and coupled synchronization loops [19]. A production flow process used in our actual processes is regarded as the coupled synchronization loops reported in Fujisaka's reference [19]. Here, we apply their model to a relatively simple cascaded system, and model the dynamics using their derived Fokker-Planck equation (FPE). The FPE applies the modulation content of the equilibrium solution to the operator as the stochastic variation, and seeks the response and correlation functions. In their numerical calculations, Fujisaka and colleagues obtained the output signal-to-noise ratio, but did not calculate the eigenvalues and eigenfunctions of the operators in the fluctuating solution.

As described above, we consider that the noise (stochastic component) in workers' capability follows a probability distribution. We study the relationship between the intensity of SR (volatility in workers' ability) and the throughput (lead time) by capturing the process as a type of threshold reaction element. The proposed concept can potentially lead to innovative productivity by companies implementing a production system. Although the test system is small, it contains useful data for analyzing an innovative production system.

This study is a continuation of a previous research manuscript on stochastic resonance (SR) [20]. We utilize a Langevin-type equation because we need to describe the mathematical model of production flow and the relation between potential energy and fluctuations [6]. In previous research, we reported that the phase difference between stages in a process corresponds to the volatility of the working time and that the parameters of the potential energy function can affect the stabilization of the process [15]. Assumptions of this paper are as follows.

- One of the processes flows sequentially next process. Moreover, there is always a worker in the production process.
- There is a correlation between the process θ_i and the upstream processes θ_{i+1} in close proximity to it in Figure 2.
- An outside company (supply chain) is regarded as delay of supply.
- Self-similarity exists in production system.

In this study, the analysis procedure of this paper is as follows.

- Consider a model of deviation signal.
- Construct a phase torus model.
- Bring into the model of Langevin type equation under self-similarity.
- Calculate the transition probability of phase torus.
- Introduce the Fokker-Planck equation after revealing the presence of stochastic resonance.
- Finally, calculate SNR after getting power spectrum.

To measure the characteristics of the coupled system, in particular for calculating the spectral density, a fundamental signal is the most important. Here, in accordance with the progress of the process, the value of autocorrelation function of elementary signal between the time t and $t + \tau$ is important.

Therefore, we are calculating the autocorrelation function of the final processes in consideration of the previous processes because the previous processes substantially affect the throughput of the final processes. The autocorrelation function is extremely important in evaluating the production flow process. When the probability intensity coefficient in the explicit solution of the autocorrelation function is small, the influence of the phase difference is small. By contrast, when the probability intensity coefficient is large, the influence is substantial and the form of the phase difference is temporally shifted in the right direction of the border. Consequently, stochastic resonance occurs. In addition, we calculate the explicit equation of the power spectrum. As a result, the correlation function spectrum of the process phase difference is known to have a Lorentz-type spectrum. Finally, we propose a mathematical model for the probability throughput. To the best of our knowledge, the explicit calculation of the autocorrelation function and its power spectrum calculation have not been previously reported.

2. **Production Framework in Equipment Manufacturer.**

The production methods used in production equipment are briefly covered in this paper. More information is provided in our report [2].

This system is considered to be a "make-to-order system with version control", which enables production after orders are received from clients, resulting in "volatility" according to its delivery date and lead time. In addition, there is volatility in the lead time, depending on the content of the make-to-order products (production equipment).

In Figure 1(A), the "Customer side" refers to an ordering company and "Supplier (D)" means the target company in this paper. The product manufacturer, which is the source of the ordered production equipment presents an order that takes account of the market

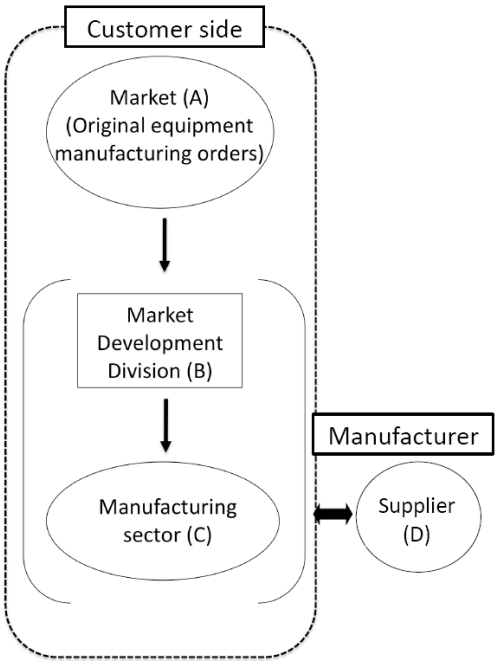

FIGURE 1. Business structure of company of research target

price. In Figure 1(B), the market development department at the customer's factory receives the order through the sale contract based on the predetermined strategy.

3. **Calculation of the Autocorrelation Function and Power Spectrum.** To measure the characteristics of the coupled system, in particular, for calculating the spectral density, we calculate the autocorrelation function of fundamental signal and power spectrum.

3.1. **Mathematical modeling by using Fokker-Plank equation.** In Figure 2, process $(i-1)$ and process $(i+1)$ are uncorrelated and θ_i denotes the phase at process i. Let the deviation of phase between processes $h_{i-1} = \theta_{i-1} - \theta_i$ and $h_i = \theta_i - \theta_{i+1}$. In Figure 3, there exists correlation between the processes proximate to one another in the production. In other words, the autocorrelation of $h_i(t)$ only is enabled. As mentioned in our previous study, the rate-of-return-deviation model in the production business can be described as a Langevin-type equation [6]. Figure 4 shows an equivalent model of flow-shop type production processes. Let $h_i \equiv d_i - d_{i-1}$ and $d\theta_i/dt = d_i$.

We call θ_i the phase parameter of the processes. A, B, C are coupling coefficients. d_i, d_{i-1} denote equivalents to the potential energies of processes. N denotes a node in the circuit. $E(t) = E_0 + e_m \sin(wt - \varphi)$ has an alternating current.

With respect to $d_i - d_{i-1} = \Delta d_i$, $\Delta d_i = 0$ basically impossible by means of the coupling coefficients A, B, C with no harmony. Therefore, the deviation signal, h_i, undergoes fluctuations. In Figure 4, asynchronous phenomena are realistically evoked in the processes due to fluctuations affected by the variable parameter C. A detailed analysis is omitted here.

h_i is represented by Langevin type equation as follows:

$$\frac{dh_i}{dt} = f_i(h_i; t) + \sqrt{H} r_i(t) \tag{1}$$

where $f_i(h_i; t)$ denotes a probability throughput. $h \in [h_1, h_2, \cdots, h_{N'}]$, and $\sqrt{H} r_i(t)$ denotes the noise term.

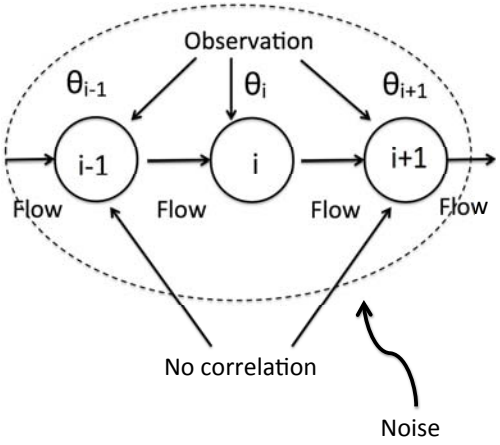

FIGURE 2. Throughput propagation under noise

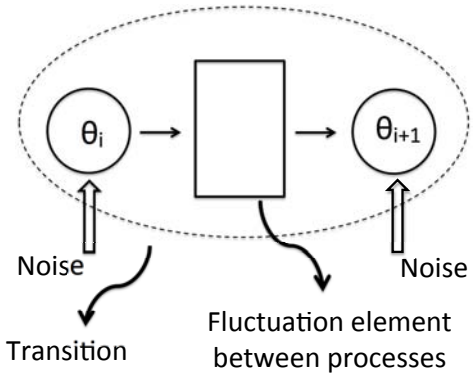

FIGURE 3. Fluctuation between processes

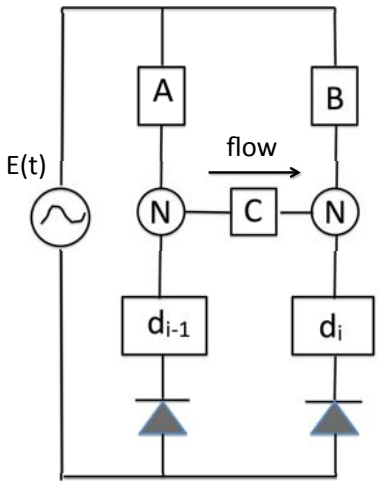

FIGURE 4. Equivalent model of throughput propagation

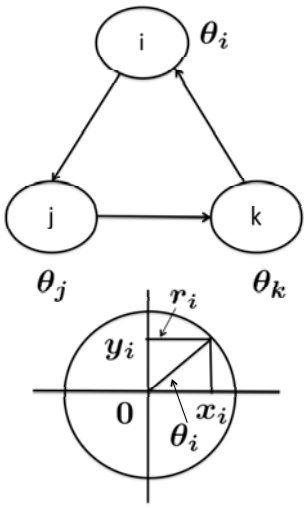

FIGURE 5. Production flow process by polar coordinate

3.2. **Calculation of the autocorrelation.** Figure 2 shows the concept of production processes. $\theta_i(t)$ denotes the output of the phase level [19].

$$\frac{d\theta_i}{dt} = -\sin M\theta_i(t) - g(t)\sin\theta_i(t) \tag{2}$$

where $\sin M\theta_i(t)$ denotes a basic cycle item ($M = 2, 4$) and $g(t)\sin\theta_i(t)$ denotes a modulation item [19].

From Equation (2), the potential energy is defined as follows [19].

Definition 3.1. *Potential energy* $V(\theta)$

$$V(\theta) = -K\left\{\sum_i \cos\theta_i + a\sum_i\sum_j \cos(\theta_i - \theta_{i+j})\right\} \tag{3}$$

Equation (3) denotes the case where no external force. Thus, to implement the characteristics as a coupled system, i.e., to calculate a spectral density, understanding the fundamental signal is important. In this study, we are interested in the value of the autocorrelation function between the time t and $t+\tau$ of a fundamental signal $\sin\theta_i$. Accordingly, we must calculate as follows to determine the potential function Equation (3).

$$< \sum_i \sin\theta_i, \sum_i \sin\theta_i^{'} > \tag{4}$$

Equation (4) represents that θ_i at t becomes $\theta_i^{'}$ at $t+\tau$.

Therefore, Equation (4) is derived as follows under the transition probability $P(\theta, t+\tau|\theta_i^{'}, t)$.

Definition 3.2. *Autocorrelation function between the time t and $t+\tau$.*

$$K_{ss}(\tau) = \int_T \int_T \left\{ \sum_i \sin\theta_i \right\} P(\theta, t+\tau|\theta_i^{'}, t) \times \left\{ \sum_i \sin\theta_i^{'} \right\} W_{st}(\theta) d\theta d\theta^{'} \tag{5}$$

where T denotes a torus.

This time, let $P(\theta, t+\tau|\theta_i^{'}, t)$ be as follows.

$$P(\theta, t+\tau|\theta_i^{'}, t) = \exp\{\mathcal{L}\cdot\tau\}\delta(\theta-\theta^{'}) \tag{6}$$

where $\mathcal{L} \approx \left(-\frac{\partial}{\partial\theta_i}\cdot H + H\cdot\frac{\partial^2}{\partial\theta_i^2}\right)$.

Hence, let $\delta(\theta-\theta^{'})$ be assumed as follows.

Assumption 3.1. *$\delta(\theta-\theta^{'})$ constitutes a complete orthonormal system.*

$$\delta(\theta-\theta^{'}) = \sum_i \varphi_i(\theta)\varphi_i(\theta^{'}) = \exp\left[\frac{1}{2}\left\{V(\theta)+V(\theta^{'})\right\}\right] \sum_i \varphi_i(\theta)\varphi_i(\theta^{'}) \tag{7}$$

Therefore, Equation (6) is derived as follows [19]:

$$P(\theta, t+\tau|\theta_i^{'}, t) = \exp\{\mathcal{L}\cdot\tau\} \times \exp\left[\frac{1}{2}\left\{V(\theta)+V(\theta^{'})\right\}\right] \sum_i \varphi_i(\theta)\varphi_i(\theta^{'}) \tag{8}$$

Hence, the autocorrelation function $K_{ss}(\tau)$ is derived as follows [19]:

$$K_{ss}(\tau) = C_{st} \sum_i \exp(\lambda_i\tau) \times \left\{ \int_T \sin\theta\varphi_i(\theta) d\theta \right\}^2 \tag{9}$$

where C_{st} denotes a normalization constant.

3.3. **Calculation of constraint equation of a synchronous system in the vicinity of the model.** The production density function $W(\varphi, t)$ is derived as follows [1]:

$$\frac{\partial W(\varphi,t)}{\partial t} + F\frac{\partial W(\varphi,t)}{\partial\varphi} = H\frac{\partial^2 W(\varphi,t)}{\partial\varphi^2} \tag{10}$$

We can obtain the eigenvalues $\phi_i(\varphi)$ and eigenfunctions λ_i by normalizing Equation (10) [1]. In Subsection 3.3, we assume Figure 6.

The variable θ in Equation (9) replaces φ.

$$K_{ss}(\tau) = C_{st} \sum_i \exp(\lambda_i\tau) \times \left\{ \int_T (\sin\varphi)\phi_i(\varphi) d\varphi \right\}^2 \tag{11}$$

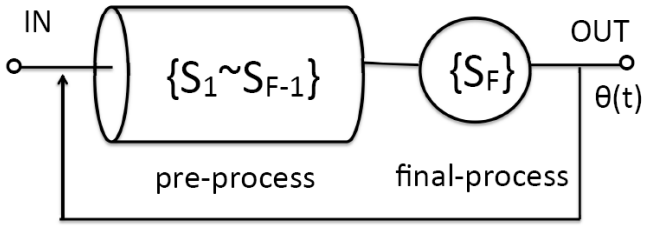

FIGURE 6. Concept of pre-process and final-process

Equation (11) denotes an autocorrelation function with respect to φ at the final process that takes account of the influence of the pre-process.

The eigenfunction $\phi_i(\varphi)$ and eigenvalue λ_i obtained by normalizing Equation (10) are derived as follows [1]:

$$\begin{aligned}
\lambda_i &= \frac{\mu}{4} + \frac{\alpha_i^2}{\mu} \\
A_i &= \left\{ 2\left(\frac{\alpha_i^2}{\mu^2} + \frac{1}{\mu} + \frac{1}{4} \right) \right\}^{\frac{1}{2}} \\
\cot \alpha_i &= \frac{\alpha_i^2}{\mu} - \frac{\mu}{4\alpha_i} \\
\phi_i(\varphi) &= A_i e^{\left(\frac{\mu}{2}\right)\varphi} \left\{ \left(\frac{2\alpha_i}{\mu} \right) \cos \alpha_i \varphi + \sin \alpha_i \varphi \right\}
\end{aligned} \tag{12}$$

Hence, $K_{ss}(\tau)$ can be calculated from Equations (11) and (12); that is, $K_{ss}(\tau)$ is derived by calculation as described in Appendix A: then, let Ψ be as follows:

$$\Psi = \left[A_i \left\{ \left(\frac{2\alpha_i}{\mu} \right) \left(\Phi^C_{(1+\alpha_i)} + \Phi^C_{(1-\alpha_i)} \right) + \Phi^S_{(1+\alpha_i)} + \Phi^S_{(1-\alpha_i)} \right\} \right]^2 \tag{13}$$

Hence, with respect to Ψ in Equation (13), $K_{ss}(\tau)$ is derived as follows:

$$K_{ss}(\tau) = C_{st} \cdot \Psi \exp(-\lambda\tau) \tag{14}$$

Therefore, the power spectrum $S_{w_n}(f)$ is as follows:

$$S_{w_n}(f) = \int_0^\infty \cos(2\pi f \cdot t) K_{ss}(t) dt \tag{15}$$

Then, letting $\lambda = \frac{1}{\tau_m}$, K_{ss} is replaced as follows:

$$K_{ss}(\tau) = C_{st} \cdot \Psi \exp\left(-\frac{t}{\tau_m} \right) \tag{16}$$

where τ_m denotes a time constant.

Accordingly, $S_{w_n}(f)$ is derived as follows:

$$\begin{aligned}
S_{w_n}(f) &= \int_0^\infty \cos(2\pi f \cdot t) K_{ss}(t) dt = \int_0^\infty \cos(2\pi f \cdot t) C_{s_t} \cdot \Psi \exp\left(-\frac{t}{\tau_m} \right) dt \\
&= C_{st} \cdot \Psi \int_0^\infty \exp\left(-\frac{t}{\tau_m} \right) \cos(2\pi f \cdot t) dt
\end{aligned} \tag{17}$$

Then, Let $\xi_t = \frac{t}{\tau_m}$. Consequently, we can obtain $dt = \tau_m d\xi_i$. Hence, $S_{w_n}(f)$ is derived as follows [14]:

$$S_{w_n}(f) = C_{st} \cdot \Psi \int_0^{\infty} \exp(-\xi_i) \cos(2\pi f \cdot \xi_i \tau_m) d\xi_i = C_{st} \cdot \Psi \left[\frac{\tau_m}{1 + (2\pi f \tau_m)^2} \right] \tag{18}$$

In the aforementioned description, if the potential function $V(\theta)$ is assumed to be a first-order approximation near the origin of θ, the power spectrum $S_{w_n}(f)$ can be obtained as Equation (18) with respect to θ.

Then, with respect to the phase difference set to φ between the pre-processes and final process, Equation (10) is derived.

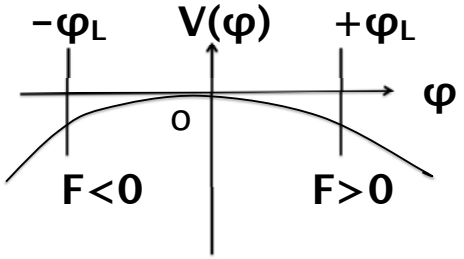

FIGURE 7. First-order approximation near the origin of θ

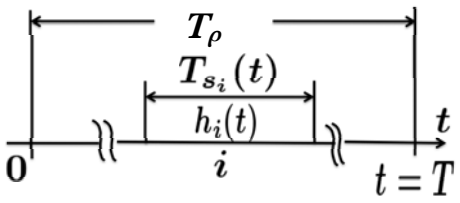

FIGURE 8. Conceptual model of the process cycle period and duration $T_{s_i}(t)$ and $T_\rho(t)$

3.4. **Phase, frequency and power spectrum.** According to our previous report [14], the coupled normal distribution $W_{\rho_i}(t)$ is derived with a first-order moment as follows:

$$r_{W_{\rho_i}}(t - t') = \frac{rI}{2} \exp\left[-r|t - t'| \right] \tag{19}$$

$W_{\rho_i}(t)$ has a normal distribution, and when its first-order moment is denoted as Equation (19), the correlation function spectrum of the phase difference in processes has been shown to have a Lorentzian spectrum [14, 22]. Furthermore, as $W_{\rho_i}(t)$ has a similar content as a process throughput, the probability throughput $C(x,t)$ is derived as follows:

$$\frac{\partial C(x,t)}{\partial t} + v \frac{\partial C(x,t)}{\partial x} = D \frac{\partial^2 C(x,t)}{\partial x^2} + Z(x,t) \tag{20}$$

where $Z(x,t)$ denotes a white noise, v is an advection speed and D is a diffusion coefficient.

Here, assuming that $C(t)$ $(\approx h(W_{\rho_i} : t \geq 0))$ is restricted to a function of time, it can be obtained, as described in our previous report, as follows [2].

$$dC(t) = \mu C(t) dt + \sigma C(t) dB(t) \tag{21}$$

where μ is a trend coefficient, σ denotes a volatility and $B(t)$ denotes a Winner process.

We can obtain a different equation as follows:

$$\frac{dC(t)}{dt} + rC(t)dt = \sqrt{H} r(t) \tag{22}$$

where r is a viscosity coefficient, and $\sqrt{H} r(t)$ is random external force.

The actual data of a test run are clarified, such as in Equations (21) and (22), from the actual data of test runs in production flow processes. Please refer to our previous report for a detailed description [12].

Next, we attempt to calculate the spectral density from Equation (10) [14, 21]. We rewrite Equation (10) as follows:

$$\frac{\partial W(\varphi,t)}{\partial t} + F\frac{\partial W(\varphi,t)}{\partial \varphi} = H\frac{\partial^2 W(\varphi,t)}{\partial \varphi^2} \tag{23}$$

In Equation (10), we define the function $W_n(t)$ with respect to time t.

Definition 3.3. *The function $W_n(t)$ with respect to time t in $H^2(D)$ space.*

$$W_n(t) = \int W(\varphi,t)\phi_n(\varphi)d\varphi \tag{24}$$

where $\phi_n(\varphi)$ denotes an eigenfunction described above.

$W_n(t)$ is satisfied as follows:

$$\frac{W_n(t)}{dt} + \Gamma_n W_n(t) = f_n(t), \quad n = 1, 2, \cdots \tag{25}$$

where Γ_n denotes a normalization constant and $f_n(t) = \sqrt{H}r_n(t)$.

Equation (23) is a diffusion equation on a dual flat space. Therefore, Equation (24) has eigenvalues and its solution is derived formally as follows:

$$W_n(t) \approx \exp\left[-\Gamma_n \cdot t\right] \cdot \Gamma_n W_n(0) + \Gamma_n \int_0^t dt' \exp\left[-\Gamma_n(t-t')\right] \cdot W_n(0) \tag{26}$$

Consequently, from Equation (26),

$$\begin{aligned} < |W_n(t)|^2 > = & \exp\left[-\Gamma_n \cdot t\right] \cdot < |W_n(0)|^2 > \\ & + < \left| \int_0^t dt' \exp\left[-\Gamma_n(t-t') \cdot \Gamma_n^{-1} W_n(t')\right] \right|^2 > \end{aligned} \tag{27}$$

where $< f_n(0) >= 0$ and $< f_n^m(t) \cdot f_n^m(t') >= 2H_f\delta_{mm'}(t-t')$.

Hence, the autocorrelation function $\phi_{W_n}(t)$ is derived according to Equation (16) as follows:

$$\phi_{W_n}(t) = H_f < |W_n|^2 > \cdot \exp\left[-\frac{t}{\tau_n}\right] \tag{28}$$

where τ_n denotes a time constant.

Consequently, the power spectral density S_{W_n} can be calculated as follows [14]:

$$S_{W_n}(f_\rho) = < |W_n|^2 > \cdot \frac{H_f \tau_n}{(2\pi f_\rho \tau_n)^2 + 1} \tag{29}$$

where

$$S_{W_n}(f_\rho) \cong \int_0^\infty \cos(2\pi f_\rho \cdot t)\phi_{W_n}(t)dt \tag{30}$$

$$\phi_\tau(t) \cong \int_0^\infty \cos(2\pi f_\rho \cdot t) S_{W_n}(f_\rho) df_\rho \tag{31}$$

Thus, $S_{W_n}(f_\rho)$ has f_ρ^{-1} characteristics. Therefore, the SNR of theoretical equation is derived as follows:

Definition 3.4. *Theoretical equation of SNR*

$$SNR \equiv \left[\frac{T_s \cdot < S_{W_n}(f_\rho) >}{S_N}\right]^2 \cdot \exp\left[-\frac{T_s}{S_N}\right] \tag{32}$$

where S_N and T_s denote a power spectrum and a threshold value respectively.

The SNR of the production flow process is

$$SNR \equiv \frac{< S_{h_n}(f_{req}) >}{S_N} \tag{33}$$

4. Numerical Simulation.

4.1. **Calculation of SNR.** The evaluation of theoretical equation (Equation (32)) and approximation equation (from actual data) is represented as follows.

(1) According to that the time constant (τ) of autocorrelation function increases, the spectral peak value is shifted to the left (See Figures 9-12, Figures 13-16, Table 1 and Table 2). There are so many situations that are over the standard working time, and it

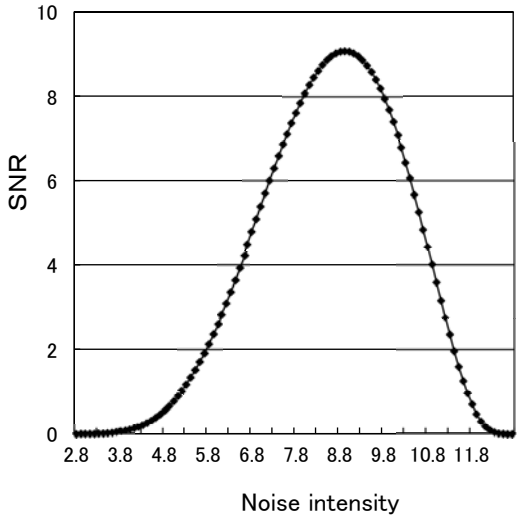

FIGURE 9. Stochastic resonance (Equation (32)), $D_\rho = 1$, $\tau = 0.5$, $T_s = 12.2$

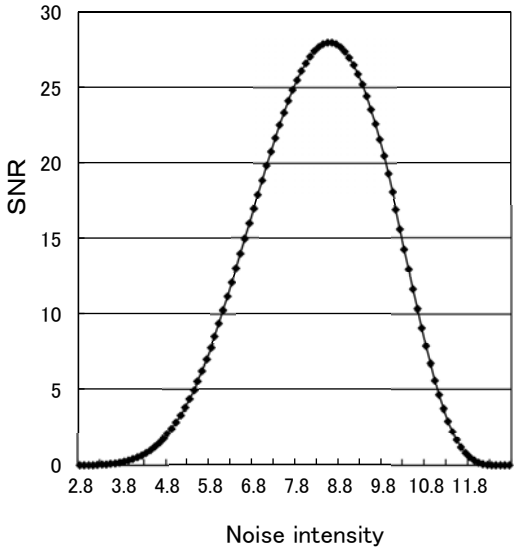

FIGURE 10. Stochastic resonance (Equation (32)), $D_\rho = 1$, $\tau = 1$, $T_s = 14$

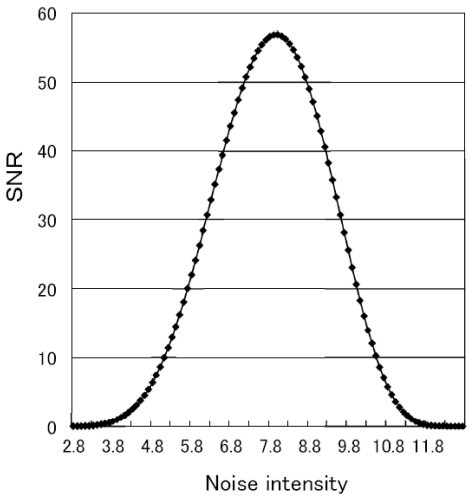

FIGURE 11. Stochastic resonance (Equation (32)), $D_\rho = 1$, $\tau = 2$, $T_s = 17.0$

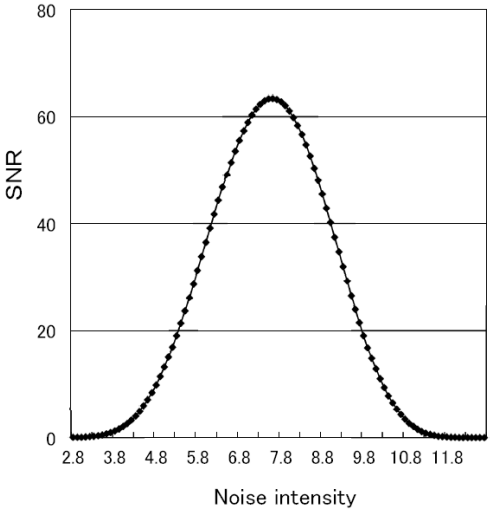

FIGURE 12. Stochastic resonance (Equation (32)), $D_\rho = 1$, $\tau = 3$, $T_s = 20$

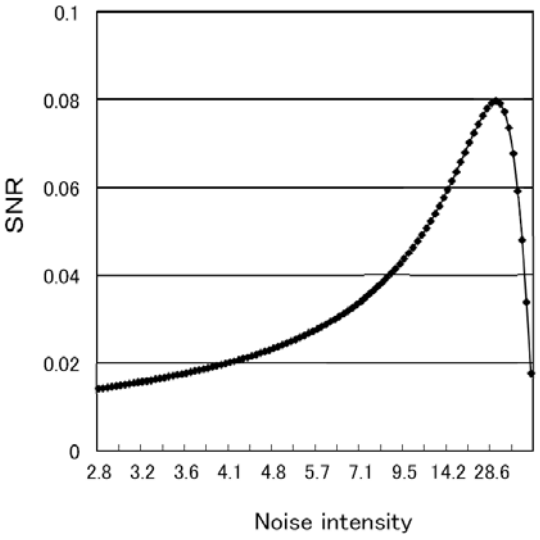

FIGURE 13. Stochastic resonance (Equation (33)), $D_\rho = 1$, $\tau = 0.5$

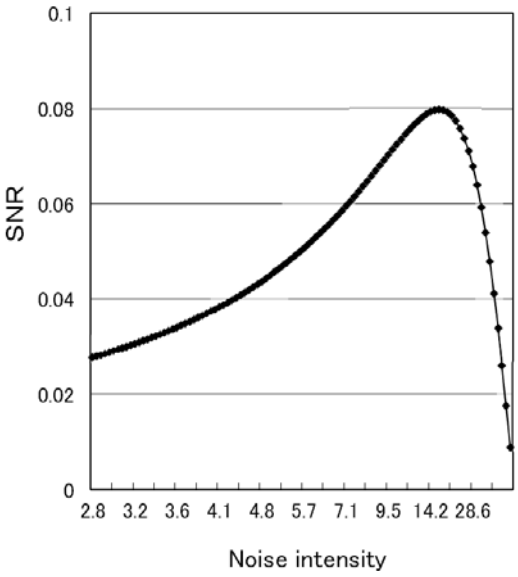

FIGURE 14. Stochastic resonance (Equation (33)), $D_\rho = 1$, $\tau = 1$

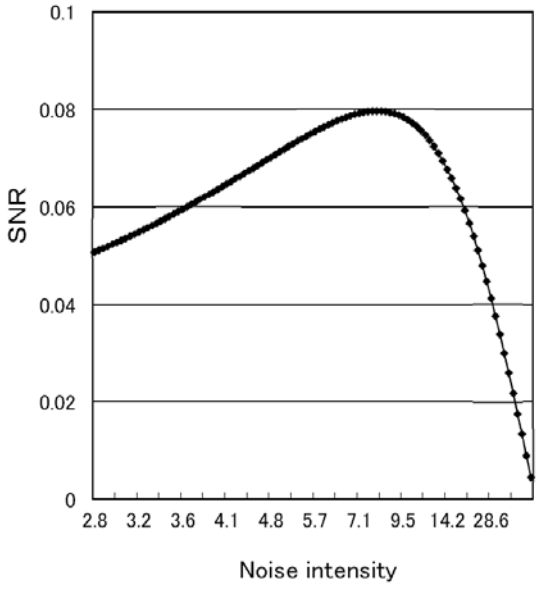

FIGURE 15. Stochastic resonance (Equation (33)), $D_\rho = 1$, $\tau = 2$

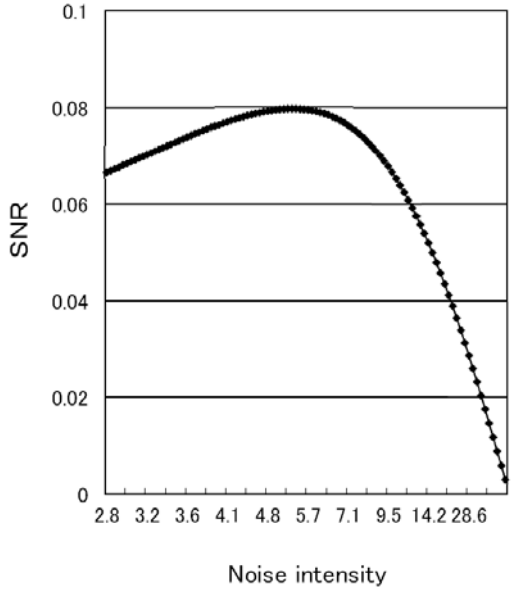

FIGURE 16. Stochastic resonance (Equation (33)), $D_\rho = 1$, $\tau = 3$

is corresponding to Figure 9/Figure 10, Figure 13/Figure 14, Figure 17/Figure 18 and Table 4 which is an asynchronous process (Test run 1). A synchronous processes (Test runs 2 and 3) indicate Figure 11/Figure 12, Figure 15/Figure 16, Figure 19/Figure 20 and Table 6/Table 8. In other words, the stochastic resonance occurs in Figure 11/Figure 12, Figure 15/Figure 16, Figure 19/Figure 20 and Table 6/Table 8.

(2) The value of SNR is larger at $T_s \approx 17$ or 20 from our theory and makes greater at $T_s \leq 20$.

When the probability intensity coefficient in the explicit solution of the autocorrelation function is small, the influence of the phase difference is small. By contrast, when the

TABLE 1. Transition of noise intensity peak value on stochastic resonance (Equation (32))

Figure number	Time constant vakue τ	SNR value	Noise intensity
Figure 9	$\tau = 0.5$	9	8.85
Figure 10	$\tau = 1.0$	27	8.8
Figure 11	$\tau = 2.0$	57	7.85
Figure 12	$\tau = 3.0$	63	7.8

TABLE 2. Transition of noise intensity peak value on stochastic resonance (Equation (33))

Figure number	Time constant value τ	SNR value	Noise intensity
Figure 13	$\tau = 0.5$	0.08	28.6
Figure 14	$\tau = 1.0$	0.08	21.4
Figure 15	$\tau = 2.0$	0.08	8.3
Figure 16	$\tau = 3.0$	0.08	5.7

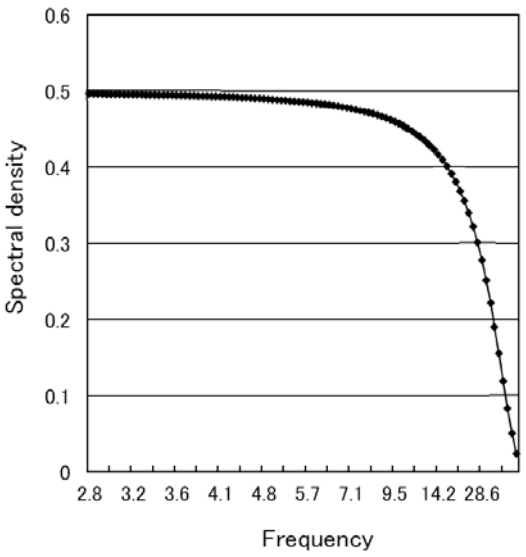

FIGURE 17. Spectral density of throughput deviation, $D_\rho = 1$, $\tau = 0.5$

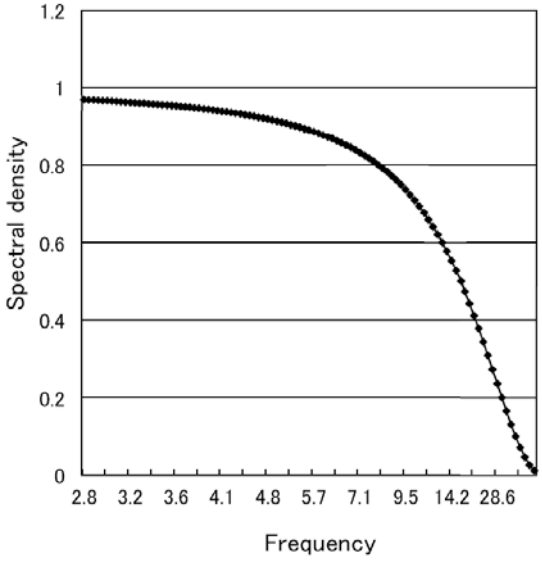

FIGURE 18. Spectral density of throughput deviation, $D_\rho = 1$, $\tau = 1$

probability intensity coefficient is large, the influence is substantial and the form of phase difference temporally is shifted in the right direction of the border. The stochastic resonance is observed to occur. That is, the stochastic resonance is clear from Figures 21 and 22 obtained by calculating Equation (23) for the transition probability density function $W(\varphi, t)$. We confirmed stochastic resonance in a test run of a production flow system. The threshold was set to $T_s \approx 20$.

Stochastic resonance can occur via the following mechanism. First, if the threshold is varied, the noise intensity amplifies in response to the large uncertainties in the overall system and human factors. Consequently, the thresholds are always exceeded and stochastic resonance is not observed. However, stochastic resonance emerges when each process is assigned the same threshold $T_s \approx 20$. The threshold response pulses that generate stochastic resonance are enclosed in the round-shaped boxes in Tables 4, 6, and

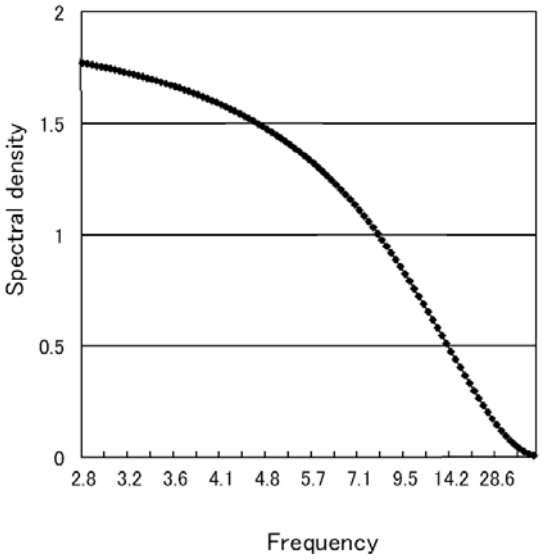

FIGURE 19. Spectral density of throughput deviation, $D_\rho = 1$, $\tau = 2$

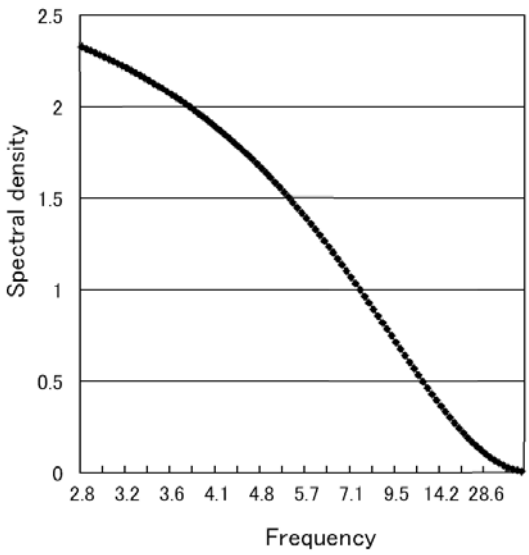

FIGURE 20. Spectral density of throughput deviation, $D_\rho = 1$, $\tau = 3$

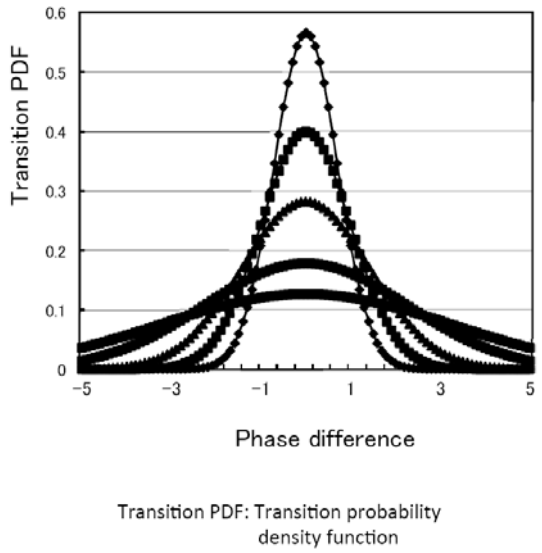

FIGURE 21. Transition probability density function (Diffusion coefficient = 0.5)

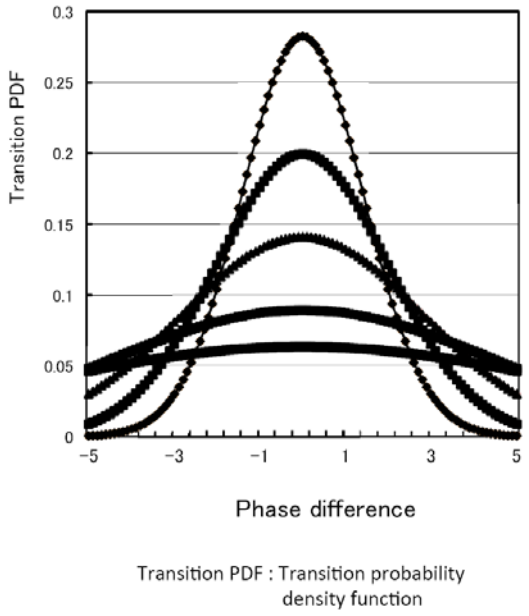

FIGURE 22. Transition probability density function (Diffusion coefficient = 2)

8. Thus, with respect to the volatility of working time in Appendix B, Table 4 shows many volatilities of data, the next is Table 6 and the minimum is a Table 8. Actual data indicate that Test run 1 is larger than Test runs 2 and 3. Please refer to the reference with respect to the actual data [11, 16].

We can get the reasonable throughput criterion value (process criterion value), which sets a 20 minute per process by setting the time constant τ to 3, from Equation (32) (Theoretical SNR) and Equation (33) (SNR of production flow process). Here, the 20 minute per process denotes "WS" of Table 6 and Table 8 in Appendix B.

TABLE 3. Correspondence between the Test-run number

	Production process	Working time	Volatility
Test run 1	Asynchronous process	627 (min)	0.29
Test run 2	Synchronous process	500 (min)	0.06
Test run 3	"Synchronization with preprocess" method	470 (min)	0.03

When a time constant is large, the fluctuation speed becomes slow. Conversely, when a time constant is small, the production throughput becomes unstable state. The optimal throughput criterion is determined by both of theoretical SNR and SNR of production flow process. Thus, we choose the value of the time constant to 0.5, 1, 2, 3.

4.2. **Actual data example of production flow process.** The production throughput is evaluated using the number of equipment pieces in comparison with the target number of equipment pieces (production ranking) and simulating asynchronous and synchronous production. The asynchronous method is prone to worker fluctuations imposed by various delays, whereas worker fluctuations in the synchronous method are small. The productivity ranking tests indicate that Test run 3 > Test run 2 > Test run 1, where Test run 1 is asynchronous and test runs 2 and 3 are synchronous. Please refer to our report for more information [16].

Here, the throughput values calculated from the throughput probability in Test run 1 – Test run 3 are as follows [16]. With respect to the actual data, please see Appendix B.

- Test run 1: 4.4 (pieces of equipment)/6 (pieces of equipment) = 0.73
- Test run 2: 5.5 (pieces of equipment)/6 (pieces of equipment) = 0.92
- Test run 3: 5.7 (pieces of equipment)/6 (pieces of equipment) = 0.95

5. **Conclusion.** We calculated the autocorrelation function of the final processes with consideration of the previous processes because the previous processes substantially affect throughput in the final processes. We adopted this approach because we needed to evaluate the production flow process. When the probability intensity coefficient in the explicit solution of the autocorrelation function is small, the influence of the phase difference is small. By contrast, when the probability intensity coefficient is large, the influence is substantial and the form of the phase difference is temporally shifted in the right direction of the border. From the actual data, we observed that the stochastic resonance occurred.

With regard to equipment manufacturing of small-to-medium-sized firm, to determine the reference value, conventionally, we have set based on the experience. To verify the reference value, we think a good way as a logical approach in that sense. Another approach is not found so far.

REFERENCES

[1] K. Shirai and Y. Amano, Prduction density diffusion equation and production, *IEEJ Trans. Electronics, Information and Systems*, vol.132-C, no.6, pp.983-990, 2012.

[2] K. Shirai and Y. Amano, A study on mathematical analysis of manufacturing lead time – Application for deadline scheduling in manufacturing system –, *IEEJ Trans. Electronics, Information and Systems*, vol.132-C, no.12, pp.1973-1981, 2012.

[3] K. Shirai and Y. Amano, Model of production system with time delay using stochastic bilinear equation, *Asian Journal of Management Science and Applications*, vol.1, no.1, pp.83-103, 2015.

[4] K. Shirai, Y. Amano and S. Omatu, Process throughput analysis for manufacturing process under incomplete information based on physical approach, *International Journal of Innovative Computing, Information and Control*, vol.9, no.11, pp.4431-4445, 2013.

[5] K. Shirai, Y. Amano, S. Omatu and E. Chikayama, Power-law distribution of rate-of-return deviation and evaluation of cash flow in a control equipment manufacturing company, *International Journal of Innovative Computing, Information and Control*, vol.9, no.3, pp.1095-1112, 2013.
[6] K. Shirai and Y. Amano, Self-similarity of fluctuations for throughput deviations within a production process, *International Journal of Innovative Computing, Information and Control*, vol.10, no.3, pp.1001-1016, 2014.
[7] K. Shirai, Y. Amano and S. Omatu, Consideration of phase transition mechanisms during production in manufacturing processes, *International Journal of Innovative Computing, Information and Control*, vol.9, no.9, pp.3611-3626, 2013.
[8] K. Shirai and Y. Amano, Calculating phase transition widths in production flow processes using an average regression model, *International Journal of Innovative Computing, Information and Control*, vol.11, no.3, pp.1075-1097, 2015.
[9] K. Shirai and Y. Amano, On-off intermittency management for production process improvement, *International Journal of Innovative Computing, Information and Control*, vol.11, no.3, pp.815-831, 2015.
[10] S. J. Baderstone and V. J. Mabin, A review Goldratt's theory of constraints (TOC) – Lessons from the international literature, *Operations Research Society of New Zealand the 33rd Annual Conference*, University of Auckland, New Zealand, 1998.
[11] K. Shirai, Y. Amano and S. Omatu, Improving throughput by considering the production process, *International Journal of Innovative Computing, Information and Control*, vol.9, no.12, pp.4917-4930, 2013.
[12] K. Shirai and Y. Amano, Production throughput evaluation using the Vasicek model, *International Journal of Innovative Computing, Information and Control*, vol.11, no.1, pp.1-17, 2015.
[13] K. Shirai, Y. Amano and S. Omatu, Propagation of working-time delay in production, *International Journal of Innovative Computing, Information and Control*, vol.10, no.1, pp.169-182, 2014.
[14] K. Shirai and Y. Amano, Application of an autonomous distributed system to the production process, *International Journal of Innovative Computing, Information and Control*, vol.10, no.4, pp.1247-1265, 2014.
[15] K. Shirai and Y. Amano, Validity of production flow determined by the phase difference in the gradient system of an autonomous decentralized system, *International Journal of Innovative Computing, Information and Control*, vol.10, no.5, pp.1727-1745, 2014.
[16] K. Shirai and Y. Amano, Analysis of production processes using a lead-time function, *International Journal of Innovative Computing, Information and Control*, vol.12, no.1, pp.125-138, 2016.
[17] R. Benzi, A. Sutera and A. Vulpiani, The mechanism of stochastic resonance, *Journal of Physics A: Mathematical and General*, vol.14, no.11, pp.453-457, 1981.
[18] S. Ishiwata and K. Koizumi, Weak signal detection and its applications by stochastic resonance, *Phenomena and Mathematical Theory of Nonlinear Waves and Nonlinear Dynamical Systems*, Reports of RIAM Symposium No.17ME-S2, 2005.
[19] H. Fujisaka, T. Kamio and K. Ikuiwa, Stochastic resonance in coupled sychronization loops, *IEICE*, vol.J90-A, no.11, pp.806-816, 2007.
[20] K. Shirai and Y. Amano, Synchronization analysis of a production process utilizing stochastic resonance, *International Journal of Innovative Computing, Information and Control*, 2016.
[21] K. Kitahara, *Nonequilibrium Statistical Mechanics*, Iwanami Co., LTD, 2000.
[22] T. Imamura, *Mathematics in Probability Field*, Iwanami Co., LTD.

Appendix A. Calculation of $\boldsymbol{K_{ss}(\tau)}$.

$$\int \sin\varphi \cdot e^{\left(\frac{\mu}{2}\right)\varphi}\left\{\left(\frac{\alpha_i}{2}\right)\cos\alpha_i\varphi + \sin\alpha_i\varphi\right\}d\varphi$$
$$= \left(\frac{\alpha_i}{2}\right)\int e^{\left(\frac{\mu}{2}\right)\varphi}\sin\varphi\cos\alpha_i\varphi d\varphi + \int e^{\left(\frac{\mu}{2}\right)\varphi}\sin\varphi\sin\alpha_i\varphi d\varphi \tag{34}$$

With respect to calculating Equation (34), the followings are as follows:

$$\Phi^S_{(1+\alpha_i)} = \frac{1}{2}\int e^{\left(\frac{\mu}{2}\right)\theta}\sin(1+\alpha_i)\theta d\theta$$

$$\Phi^{S}_{(1-\alpha_i)} = \frac{1}{2}\int e^{\left(\frac{\mu}{2}\right)\theta}\sin(1-\alpha_i)\theta d\theta$$
$$\Phi^{C}_{(1+\alpha_i)} = \frac{1}{2}\int e^{\left(\frac{\mu}{2}\right)\theta}\cos(1+\alpha_i)\theta d\theta$$
$$\Phi^{C}_{(1-\alpha_i)} = \frac{1}{2}\int e^{\left(\frac{\mu}{2}\right)\theta}\cos(1-\alpha_i)\theta d\theta \tag{35}$$

where

$$\Phi^{S}_{(1\pm\alpha_i)} = \frac{1}{2(1\pm\alpha_i)}\left[1+\frac{1}{\beta^3}\right]\left(\frac{1}{\beta}\right)\times\left[e^{\beta x}\sin x+\frac{1}{\beta^2}e^{\beta x}\cos x\right]_0^T \tag{36}$$

or

$$\Phi^{S}_{(1\pm\alpha_i)} = \frac{1}{2(1\pm\alpha_i)}\left[1+\frac{1}{\beta^2}\right]\left(\frac{1}{\beta}\right)\times\left[e^{\beta x}\cos x+\frac{1}{\beta^2}e^{\beta x}\sin x\right]_0^T \tag{37}$$

Then, $K_{ss}(\tau)$ is derived as follows:

$$K_{ss}(\tau) = C_{s_t}\sum_i \exp(\lambda_i\tau)\times\left[A_i\left\{\left(\frac{2\alpha_i}{\mu}\right)\left(\Phi^{C}_{(1+\alpha_i)}+\Phi^{C}_{(1-\alpha_i)}\right)+\Phi^{S}_{(1+\alpha_i)}+\Phi^{S}_{(1-\alpha_i)}\right\}\right]^2 \tag{38}$$

Appendix B. **Actual Data in the Production Flow System.** As a result, the above test-run is as follows.

- (Test-run 1) Each throughput in every process (S1-S6) is asynchronous, and its process throughput is asynchronous. Table 4 represents the manufacturing time (min) in each process. Table 5 represents the variance in each process performed by workers. Table 4 represents the target time, and the theoretical throughput is given by $3 \times 199 + 2 \times 15 = 627$ (min).

  In addition, the total working time in stage S3 is 199 (min), which causes a bottleneck. Figure 23 is a graph illustrating the measurement data in Table 4, and it represents the total working time for each worker (K1-K9). The graph in Figure 24 represents the variance data for each working time in Table 4.
- (Test-run 2) Set to synchronously process the throughput.

  The target time in Table 6 is 500 (min), and the theoretical throughput (not including the synchronized idle time) is 400 (min). Table 7 represents the variance data of each working process (S1-S6) for each worker (K1-K9).
- (Test-run 3) The process throughput is performed synchronously with the reclassification of the process. The theoretical throughput (not including the synchronized idle time) is 400 (min) in Table 8.

  Table 9 represents the variance data of Table 8. "WS" in the measurement tables represents the standard working time. This is an empirical value obtained from long-term experiments.

TABLE 4. Total manufacturing time at each stages for each worker

	WS	S1	S2	S3	S4	S5	S6
K1	15	(20)	(20)	(25)	(20)	(20)	(20)
K2	20	(22)	(21)	(22)	(21)	(19)	(20)
K3	10	(20)	(26)	(25)	(22)	(22)	(26)
K4	20	17	15	19	18	16	18
K5	15	15	(20)	(18)	(16)	15	15
K6	15	15	15	15	15	15	15
K7	15	(20)	(20)	(30)	(20)	(21)	(20)
K8	20	(29)	(33)	(30)	(29)	(32)	(33)
K9	15	14	14	15	14	14	14
Total	145	172	184	199	175	174	181

TABLE 5. Volatility of Table 4

K1	1.67	1.67	3.33	1.67	1.67	1.67
K2	2.33	2	2.33	2	1.33	1.67
K3	1.67	3.67	3.33	2.33	2.33	3.67
K4	0.67	0	1.33	1	0.33	1
K5	0	1.67	1	0.33	0	0
K6	0	0	0	0	0	0
K7	1.67	1.67	5	1.67	2	1.67
K8	4.67	6	5	4.67	5.67	6
K9	0.33	0.33	0	0.33	0.33	0.33

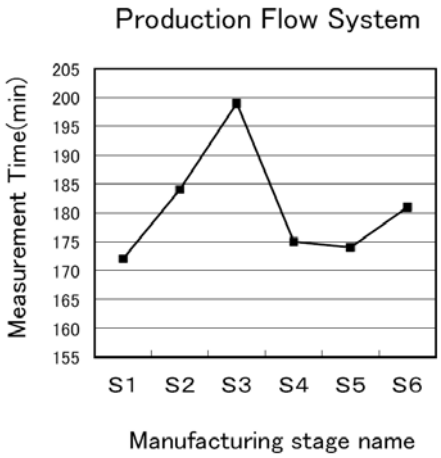

FIGURE 23. Total work time for each stage (S1-S6) in Table 4

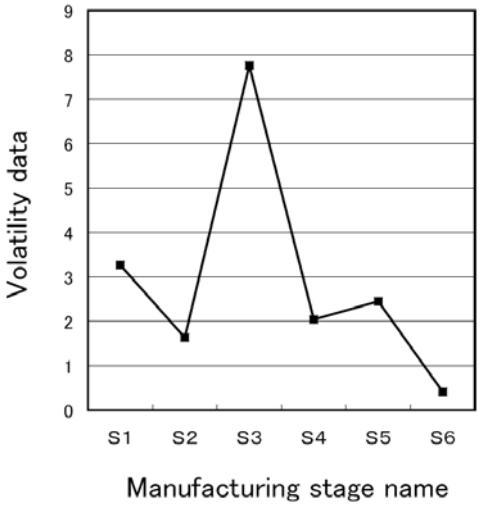

FIGURE 24. Volatility data for each stages (S1-S6) in Table 4

TABLE 6. Total manufacturing time at each stages for each worker

	WS	S1	S2	S3	S4	S5	S6
K1	20	20	(24)	20	20	20	20
K2	20	20	20	20	20	22	20
K3	20	20	20	20	20	20	20
K4	20	(25)	(25)	20	20	20	20
K5	20	20	20	20	20	20	20
K6	20	20	20	20	20	20	20
K7	20	20	20	20	20	20	20
K8	20	(27)	(27)	(22)	(23)	20	20
K9	20	20	20	20	20	20	20
Total	180	192	196	182	183	182	180

TABLE 7. Volatility of Table 6

K1	0	1.33	0	0	0	0
K2	0	0	0	0	0.67	0
K3	0	0	0	0	0	0
K4	1.67	1.67	0	0	0	0
K5	0	0	0	0	0	0
K6	0	0	0	0	0	0
K7	0	0	0	0	0	0
K8	2.33	2.33	0.67	1	0	0
K9	0	0	0	0	0	0

TABLE 8. Total manufacturing time at each stages for each worker

	WS	S1	S2	S3	S4	S5	S6
K1	20	18	19	18	20	20	20
K2	20	18	18	18	20	20	20
K3	20	(21)	(21)	(21)	20	20	20
K4	20	13	11	11	20	20	20
K5	20	16	16	17	20	20	20
K6	20	18	18	18	20	20	20
K7	20	14	14	13	20	20	20
K8	20	(22)	(22)	20	20	20	20
K9	20	(25)	(25)	(25)	20	20	20
Total	180	165	164	161	180	180	180

TABLE 9. Variance of Table 8

K1	0.67	0.33	0.67	0	0	0
K2	0.67	0.67	0.67	0	0	0
K3	0.33	0.33	0.33	0	0	0
K4	2.33	3	3	0	0	0
K5	1.33	1.33	1	0	0	0
K6	0.67	0.67	0.67	0	0	0
K7	2	2	2.33	0	0	0
K8	0.67	0.67	0	0	0	0
K9	1.67	1.67	1.67	0	0	0